

Light-responsive amphiphilic copolymer coated nanoparticles as nanocarriers and real-time monitors for controlled drug release†

Cite this: *J. Mater. Chem. B*, 2014, 2, 1182

Qingjian Xing,^a Najun Li,^{*ab} Dongyun Chen,^a Wenwei Sha,^a Yang Jiao,^c Xiuxiu Qi,^a Qingfeng Xu^{ab} and Jianmei Lu^{*ab}

Herein, light-responsive nanocarriers based on hollow mesoporous silica (HMS) nanoparticles modified with spiropyran-containing light-responsive copolymer (PRMS-FA) were fabricated via a simple self-assembly process. HMS modified with long-chain hydrocarbon octadecyltrimethoxysilane was an ideal base material owing to its good biocompatibility and drug capability. The spiropyran-containing amphiphilic copolymer could shift its hydrophilic–hydrophobic balance to become hydrophilic upon UV ($\lambda = 365$ nm) irradiation and then break away from the hydrophobic surface of the HMS core, followed by the uncaging and release of the pre-loaded anticancer drug. Simultaneously, the fluorescence resonance energy transfer (FRET) process based on the structural transformation of PRMS-FA was observed, which could act as a real-time monitor for the light-controlled drug release. Our model experiments *in vitro* tested and verified that this composite nanocarrier has good biocompatibility, active tumour targeting to the folate receptor over-expressed in tumour cells, is non-toxic to normal cells and that light-controlled drug release with real-time monitoring can be achieved.

Received 16th September 2013
Accepted 22nd November 2013

DOI: 10.1039/c3tb21269f

www.rsc.org/MaterialsB

Introduction

In recent years, nanoscale drug delivery systems (NDDS) have attracted considerable attention for their potential applications in biomedical fields.¹ Among them, polymeric micelles assembled by amphiphilic copolymers containing stimuli-responsive moieties which respond to various external stimuli, such as light, pH and temperature, have been introduced as drug carriers for controlled release.² Light, having higher selectivity in time and space than other stimuli, is considered to be an ideal trigger in NDDS.³ Some light triggered NDDS based on functional nanoparticles, upconverting nanoparticles for example, have been reported.⁴ Since good control over the reaction could be ensured by adjusting the wavelength and intensity of the light,⁵ light-triggered drug delivery systems based on polymeric micelles have been designed to be applied in controlled drug release through introduction of photochromic compounds such as azobenzene, spiropyran,

o-nitrobenzyl and coumarin.⁶ In addition, such light-responsive drug carriers could be modified by introduction of tumour targeting compounds to the polymers, such as folic acid, peptide and antibodies, to achieve active targeting ability.⁷ Hence light irradiation would disaggregate the light-responsive drug carriers to release the loaded drugs after they had gathered at the tumour site.⁸

Spiropyran, one of the photochromic compounds, exists as a closed-loop non-colored spiroform (SP) under visible light irradiation, whereas it can be converted to an open-loop colored merocyanine form (MC) under UV irradiation ($\lambda = 365$ nm). What is more, the SP form is hydrophobic and can be converted into the hydrophilic MC form by UV irradiation.⁹ So spiropyran-containing amphiphilic polymeric micelles may disaggregate owing to the structural transformation upon UV irradiation, resulting in the release of drugs pre-loaded in the micelles. This could provide a strategy to design a spiropyran-based light-responsive nanocarrier for light-controlled drug delivery and release.

In controlled drug release systems, real-time monitoring of the drug release plays an important role. The fluorescence resonance energy transfer (FRET) process was confirmed to act as a monitor in drug nanocarriers based on the energy transfer between coumarin and FITC.¹⁰ Such a strategy was also suitable for application in a light-controlled drug release system. Spiropyran, could act as the acceptor in the FRET process while rhodamine B, a common fluorescent compound, can be used as the donor owing to their well matching absorption and

^aJiangsu Key Laboratory of Advanced Functional Polymer Design and Application, College of Chemistry, Chemical Engineering and Materials Science, Soochow University, Suzhou, 215123, China. E-mail: linajun@suda.edu.cn; lujm@suda.edu.cn; Fax: +86-512-6588-0367; Tel: +86-512-6588-0367

^bState Key Laboratory of Treatments and Recycling for Organic Effluents by Adsorption in Petroleum and Chemical Industry, Suzhou, 215123, China

^cSchool of Radiation Medicine and Protection, Medical College of Soochow University, Suzhou, Jiangsu 215123, China

† Electronic supplementary information (ESI) available: Experimental section. See DOI: 10.1039/c3tb21269f

emission bands.¹¹ In the FRET process, the open-loop MC form of spiropyran has a strong overlap and quenches the fluorescence of rhodamine B upon UV irradiation while the SP form does not. Therefore, it is possible that an amphiphilic copolymer containing both spiropyran and rhodamine B moieties can show a similar FRET process after UV irradiation. Since the FRET process occurred simultaneously with the disaggregation of polymeric micelles upon UV irradiation, it could act as a real-time monitor for light-triggered drug release based on changes in the fluorescence signal.

To improve the drug-loading capability and morphological stability of polymeric micelles, some functional inorganic nanoparticles were incorporated into the micelles by a self-assembly process.¹² This strategy could combine the beneficial properties of the inorganic nanoparticles with polymeric micelles for better application in drug delivery.¹³ Among such inorganic nanoparticles, hollow mesoporous silica (HMS) nanoparticles are ideal base materials with high biocompatibility and drug loading capability.¹⁴ Besides, the nanoparticles can be easily modified owing to the large amount of Si-OH on the outer surface. To achieve a "smart" controlled drug release system, HMS nanoparticles are usually coated with stimuli-responsive polymer and such composite construction was confirmed to be stable without external stimulus according to our previous work.^{15,16}

Here we designed a spiropyran-containing light-responsive amphiphilic copolymer which was coated onto the surface of HMS nanoparticles forming a drug nanocarrier (Scheme 1). Firstly, a spiropyran-containing amphiphilic copolymer, poly-(RBM-MAPEG-SPMA) (PRMS), was synthesized by radical copolymerization. Poly(ethylene glycol) (PEG), a popular hydrophilic polymer with good biocompatibility and stealth behaviour, was introduced as the hydrophilic part. Folic acid (FA), a common tumour targeting compound for tumour cells with over-expressed folate receptors (FR(+)), was then conjugated with the PRMS to achieve the final multifunctional copolymer, PRMS-FA. Hollow mesoporous silica (HMS) nanoparticles with high drug loading capacity acted as the drug delivery matrix to be modified with the light-responsive

targeting copolymer PRMS-FA *via* a simple self-assembly process. Hence the core-shell light-triggered nanocomposites for targeting drug delivery and controlled release were obtained. We mainly investigated light controlled drug release under UV ($\lambda = 365$ nm) irradiation and the possibility of the fluorescence resonance energy transfer (FRET) process being used as the real-time monitor for pre-loaded drug release.

Experimental section

Materials

2,3,3-Trimethyl-3*H*-indol, 2-hydroxy-5-nitrobenzaldehyde and 2-bromoethanol were purchased from TCI. (2-(Acryloyloxy) ethyl) trimethylammonium chloride (AETAC, 80 wt% in water), 2,2'-azobis(2-methylpropionamide) dihydrochloride (V-50, >97.0%), octadecyltrimethoxysilane (C18), hexadecyltrimethylammonium bromide (CTAB, >99%) and poly(ethylene glycol) methacrylate (MAPEG, M_n average = 526) were all purchased from Aldrich. Folic acid, methacryloyl chloride, methanesulfonyl chloride, sodium azide, triphenylphosphine were all purchased from Shanghai Chemical Reagent Co. Ltd. Rhodamine B, *N*-hydroxysuccinimide (NHS, 99%) and dicyclohexacarbodiimide (DCC, 99%) were purchased from Alfa Aesar.

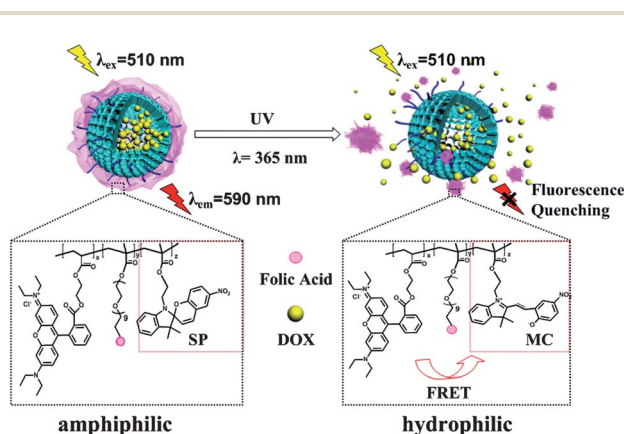
Modification of HMS with C18 (HMS@C18)

First, the hollow mesoporous silica (HMS) nanoparticles were synthesized according to the literature with some modifications.¹⁵ Then, 100 mg HMS nanoparticles were dispersed in 20 mL anhydrous acetonitrile before 5 mL C18 was added. The obtained suspension was stirred for 24 h and collected by centrifugation, washed with acetonitrile and ethanol several times, and dried under vacuum for further usage.

Synthesis of hydrophobic monomer 1'-(2-methacryloxyethyl)-3',3'-dimethyl-6-nitro-spiro(2*H*-1-benzopyran-2',2'-indoline) (SPMA)

The synthetic route to SPMA is shown in Scheme S1.† SPOH was synthesized according to the literature.¹⁷ The general procedure employed for the preparation of SPMA is as follows. SPOH (1.0 g, 2.84 mmol) was dissolved in dry CH_2Cl_2 (15 mL) and Et_3N (868 μL , 6.25 mmol) was added. The mixture was cooled to 0 °C under argon and protected against exposure to visible light. Methacryloyl chloride (550 μL , 5.68 mmol) in dry CH_2Cl_2 (5 mL) was then added dropwise over 0.5 h. The mixture was allowed to stir over night at room temperature. After the solvent was removed using a rotary evaporator, the residues were purified by silica gel column chromatography (petroleum ether- $\text{CH}_2\text{Cl}_2 = 1 : 2$) to give SPMA as a green solid (0.48 g, 40%).

¹H NMR (400 MHz, CDCl_3), δ (ppm): 7.97–8.05 (m, 2H), 7.17–7.24 (m, 1H), 7.09 (d, 1H), 6.89 (q, 2H), 6.74 (q, 2H), 6.07 (d, 2H), 5.87 (d, 1H), 5.56 (d, 2H), 4.3 (t, 2H), 3.37–3.62 (m, 2H), 1.91 (s, 3H), 1.28 (s, 3H), 1.16 (s, 3H).



Scheme 1 Schematic depiction of light controlled drug release from HMS/C18/PRMS-FA and the FRET process.

Synthesis of rhodamine B (2-hydroxyethyl acrylate) ester (RBM)

The general procedure is as follows. Rhodamine B (10 g) was dissolved in 1,2-dichloroethane (150 mL) and thionyl chloride (10 mL) was added slowly to the solution below 0 °C. Then the reaction mixture was stirred under reflux for 8 h. After cooling down to room temperature, 2-hydroxyethyl acrylate (15 mL) was added to the solution and the mixture was allowed to stir overnight. The resulting product was purified by silica gel column chromatography (CH₂Cl₂–CH₃OH = 30 : 1, v/v) to give RBM as a purple solid (510 mg, 42.2%).

¹H NMR (400 MHz, CDCl₃), δ (ppm): 8.32 (d, 1H), 7.85 (t, 1H), 7.76 (d, 1H), 7.33 (d, 1H), 7.07 (d, 2H), 6.94 (d, 2H), 6.81 (s, 2H), 6.37 (m, 1H), 6.05 (m, 1H), 5.87 (m, 1H), 4.29 (m, 2H), 4.17 (m, 2H), 3.66 (m, 8H), 1.34 (t, 12H).

Synthesis of MAPEG amine (MAPEG-NH₂)

MAPEG amine was synthesized according to the literature.¹⁸ MAPEG azide was prepared in two steps (see ESI†). Then MAPEG azide (2.76 g, 5 mmol) was dissolved in THF (5 mL). Triphenylphosphine (1.572 g, 6 mmol) was added, N₂ evolution was observed, and the mixture was stirred at room temperature for 2 h. Distilled water (0.5 mL) was added, and the mixture was stirred at room temperature overnight. The mixture was evaporated and dissolved in CH₂Cl₂. The solution was washed with 1 N HCl (twice). The aqueous layer was made basic with 1 N NaOH and extracted with CH₂Cl₂ (twice). The organic layer was dried over MgSO₄, filtered, and evaporated to give MAPEG amine as a yellow liquid (1.32 g, 50%).

¹H NMR (400 MHz, CDCl₃), δ (ppm): 6.12 (m, 1H), 5.57 (m, 1H), 4.29 (m, 2H), 3.74 (t, 2H), 3.64 (m, 32H), 3.54 (t, 2H), 1.94 (s, 3H).

Synthesis of the light-responsive copolymer poly(RBM-MAPEG-SPMA) (PRMS)

PRMS was synthesized by radical copolymerization. MAPEG amine (315.6 mg, 0.6 mmol), SPMA (84 mg, 0.2 mmol) and RBM (1.2 mg, 0.002 mmol) were dissolved in cyclohexanone (2 mL). Then, AIBN (1.1 mg) was added to the mixture. The reaction mixture was stirred at 70 °C for 12 h under argon. After that, the solution was suspended in anhydrous ether (100 mL) and the copolymer was obtained after centrifugation at 8000 rpm for 10 min. The copolymer was washed several times before being dried under vacuum for further usage.

Synthesis of folate conjugated copolymer PRMS-FA

The conjugation procedure was briefly as follows. FA-NHS was prepared at first (see ESI†). Then FA-NHS (30 mg) was added to dry pyridine containing 200 mg of the above copolymer. The solution was stirred for 12 h at room temperature (protected against visible light exposure). Then, the mixture was precipitated in 10% acetone in anhydrous ether. The copolymer PRMS-FA was obtained by centrifugation and stored in the dark at 4 °C.

Preparation of HMS@C18@PRMS-FA

HMS@C18 (5 mg) was dispersed in 1 mL tetrahydrofuran by sonication for 5 min. PRMS-FA (30 mg) was dissolved in the solution. Then, 5 mL distilled water was added dropwise to the above solution with vigorous stirring and the resulting mixture was stirred vigorously over night while the tetrahydrofuran evaporated. After that, the product was separated by centrifugation and washed with distilled water several times.

Drug loading and release experiment

To evaluate the drug loading and release properties, doxorubicin (DOX) was used as a model anticancer agent. DOX was extracted from doxorubicin hydrochloride (DOX·HCl) according to the procedure reported previously.¹⁹ HMS/C18 (8, 4 and 0.8 mg mL⁻¹) was dispersed into 1 mL phosphate buffered saline (PBS) solution, then DOX solution (5 mg mL⁻¹, 80 μL) was added. The mixture was stirred for 24 h (protected against visible light exposure). Afterwards, DOX/HMS/C18 were obtained by centrifugation and washed several times, then dried at 60 °C under vacuum.

To evaluate the amount of drug loaded into HMS/C18, UV-Vis spectroscopy was used for analysis. First, the calibration curve of DOX was determined by taking absorbance vs. DOX concentration between 0 and 5 mg L⁻¹ as parameters, and the calibration curve was fitted to the Lambert–Beer law as follows:

$$A = 0.0014 + 0.0091C$$

where *A* is the absorbance and *C* is the concentration (mg L⁻¹). After adsorption, the DOX solution (100 μL) was extracted and diluted to 10 mL, and then analyzed by UV-Vis spectroscopy at a wavelength of 485 nm. Drug loading content and drug loading efficiency can be calculated as follows:

$$\text{Drug loading content (wt\%)} = (\text{weight of loaded drug/weight of nanocomposites}) \times 100\%$$

$$\text{Drug loading efficiency (\%)} = (\text{weight of loading drug/weight of drug in feed}) \times 100\%$$

The drug release test was performed by suspending the DOX-loaded nanoparticles in phosphate buffered saline (PBS) at 37 °C. The solution was shaken vigorously under visible light and UV (λ = 365 nm) irradiation alternately. To determine the release amount at any given time, a portion of solution was withdrawn after centrifugation and the same volume PBS was added to keep the volume constant. The drug concentration in the withdrawn solution was analyzed by measuring the absorbance of DOX using UV-Vis spectroscopy.

Cell culture and preparation

Human KB cell lines with folic acid receptors (FR(+)) and A549 human alveolar adenocarcinoma cell lines without folic acid receptors (FR(-)) were purchased from Shanghai Cell Institute Country Cell Bank, China and cultured as monolayers in

RPMI-1640 medium supplemented with 10% heat-inactivated fetal bovine serum at 37 °C in a humidified incubator (5% CO₂ in air, v/v).

In vitro cytotoxicity

The aminoxanthene dye, sulforhodamine B (SRB) was used as an assay for assessing the effects of drug carriers (HMS@C18@PRMS-FA) in various concentrations. Briefly, strongly growing KB cells were placed in 96-well plates (1.3 × 10⁴ cells per well) and four duplicate wells were set up in the sample. The culture medium was replaced with a medium containing different concentrations of drug carriers and cultured at 37 °C in a humidified incubator (5% CO₂ in air, v/v) with the cells anchored to the plates. After being cultured for 72 h, the medium was poured away and 10% (w/v) trichloroacetic acid in Hank's balanced salt solution (100 mL) was added and stored at 4 °C for 1 h. Then the stationary liquid was discarded, the cells were washed with deionized water five times before air drying and stained with 0.4% (w/v) SRB solution (100 mL per well) for 30 min at room temperature. After removing the SRB, the cells were washed with 0.1% acetic acid solution five times. Bound SRB dye was solubilized with 10 mmol⁻¹ Tris-base solution (150 mL, pH = 10.5). The optical density (OD) value of each individual well was calculated by using a spectrophotometer to measure the absorbance at 531 nm.

The cell cytotoxicity of light-triggered DOX release was assessed by the standard MTT assay. To test the cytotoxicity of the DOX-loaded drug carriers with and without UV irradiation, KB cells were seeded in a 96-well plate at a density of 1.3 × 10⁴ cells per well and cultured in 5% CO₂ at 37 °C for 24 h. Then the drug carriers were added to the medium. For the drug carrier without UV irradiation, the cells were incubated for varying time durations. For the drug carrier with UV irradiation, the carrier was removed after 3 h of incubation followed by exposure to UV light. Then the cells were incubated for another 24 h in the dark. After that, the medium was removed before 100 μL MTT solution (0.5 mg mL⁻¹) was added and incubated for a further 4 h. The medium was then replaced with 100 μL DMSO per well and the absorbance was monitored using a microplate reader at a wavelength of 485 nm. The cytotoxicity was expressed as the percentage of cell viability compared to the untreated cells.

CLSM observation of the cell uptake and the FRET process

The nanocarrier is easily observed, owing to the fluorescent rhodamine B component, by confocal laser fluorescence microscopy (CLSM). For CLSM observation of the cell uptake, A549 cells and KB cells were seeded in 96-well plates (1.3 × 10⁴ cells per well) and incubated overnight at 37 °C in a humidified incubator. The sample of DOX/HMS/C18/PRMS-FA was dispersed in RPMI-1640 medium. Cells were cultured with the DOX/HMS/C18/PRMS-FA solution for a certain time and observed using CLSM after washing three times with PBS. For CLSM observation of the FRET process accompanied by DOX release under UV irradiation, the KB cells were treated with DOX/HMS/C18/PRMS-FA at the same concentration of 500 μg

mL⁻¹. The medium was removed after 3 h of incubation and the cells were washed before treatment with various UV light doses. After a further 1 h of incubation, the cells were washed and observed using CLSM at a wavelength of 510 nm.

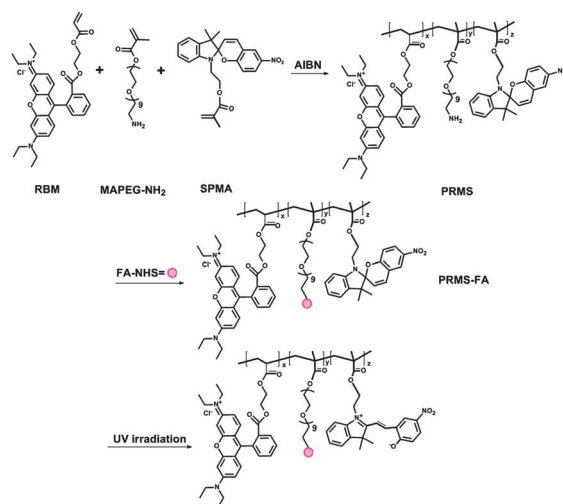
Characterization

¹H NMR spectra were measured using an INOVA 400 MHz NMR instrument. FT-IR measurements were performed using KBr pellets on a Nicolet 4700 spectrometer (Thermo Fisher Scientific) in the range of 400–4000 cm⁻¹. The UV-Vis absorption spectra were measured on a TU-1901 spectrophotometer. Fluorescence spectra were measured on a HORIBA Jobin Yvon's fluorescence spectrofluorometer. Gel permeation chromatography (GPC) analysis was carried out using a Waters 1515 pump and a differential refractometer, THF was used as the mobile phase at a flow rate of 1.0 mL min⁻¹. TEM images were obtained using a TecnaiG220 electron microscope at an acceleration voltage of 200 kV. Brunauer-Emmett-Teller (BET) and Barrett-Joyner-Halenda (BJH) analyses were used to determine the surface area, pore size and pore volume and measurements were obtained with a Quantachrome Autosorb 1C apparatus at -196 °C under continuous adsorption conditions. The UV (365 nm, 6 W) and light-emitting diode (LED) lamps (620 nm, 15 W) were used as light sources for UV and visible light irradiation. Confocal laser scanning microscopy (CLSM) images were observed by a confocal laser scanning microscopy (Olympus, FV 1000).

Results and discussion

Synthesis and FRET behaviour of PRMS-FA

The amphiphilic copolymer PRMS-FA was synthesized following the procedure shown in Scheme 2. The GPC data for the copolymers with different molar ratios is summarized in Table S1.† PRMS (*M*_n = 11 600, PDI = 1.243) was chosen to be conjugated with FA-NHS to obtain PRMS-FA (*M*_n = 16 700, PDI = 1.72). Approximately 63.7% of PEG chains on average were



Scheme 2 Schematic synthetic route to PRMS-FA.

conjugated with folic acid according to the incremental quantity of the molecular weight. The structure of PRMS-FA was confirmed by ^1H NMR (see Fig. S1†), in which the characteristic peaks in SPMA ($\delta = 4.3$ and $6.75\text{--}7.0$ ppm), RBM ($\delta = 8.10\text{--}8.16$ ppm) and folic acid ($\delta = 6.64, 7.65$ and 8.64 ppm) were all observed correspondingly, confirming that the amphiphilic copolymers PRMS-FA were synthesized successfully.

Spiropyran can be reversibly switched between the non-colored closed-loop state (SP, spiroform) and another colored open-loop state (MC, merocyanine form) by irradiation with visible light and ultraviolet light. The UV-Vis absorption of spiropyran methacrylate (SPMA) before and after irradiation with UV light at 365 nm is shown in Fig. 1a. It is worth noting that the absorption bands of SPMA match well with the emission bands of rhodamine B (2-hydroxyethyl acrylate) ester (RBM) under UV irradiation. The FRET process requires overlap of the emission bands of the donor and acceptor in general. Therefore, RBM could act as the donor while SPMA acts as the acceptor in this system. Thus, a similar FRET process is expected to occur along with the transformation of PRMS-FA from an amphiphilic copolymer to a hydrophilic polymer upon UV irradiation. The photographs and the change in fluorescence emission intensity under alternating UV and visible light irradiation shown in Fig. 1b demonstrate the process. Under visible irradiation, the bright red solution of PRMS-FA showed quite high fluorescence intensity (excited at 510 nm) which was derived from the rhodamine B moiety. Upon UV irradiation, the

non-colored spiropyran in SP form turned into the colored MC form, which resulted in the color change of copolymer solution to a much darker colour. Meanwhile, the fluorescence emission of the copolymer at 510 nm decreased significantly, which could be ascribed to the quenching of RBM fluorescence by the MC form of the SPMA moieties when the FRET process occurred. Since the amphiphilic copolymer PRMS-FA would become hydrophilic upon UV irradiation, the accompanied FRET process in the form of fluorescence quenching could provide evidence for such a transformation.

The surface of HMS was enriched with Si-OH, which could be easily modified with C18. The FT-IR spectra of HMS, HMS/C18 and DOX/HMS/C18 are shown in Fig. 2. The Si-OH bond (950 cm^{-1}) in the spectrum of HMS suggested that a large number of silanol groups existed on the surface of HMS for coupling long alkyl chains and functional molecules. As shown in the spectrum of HMS/C18, a strong band of C-H_x (2890 cm^{-1}) revealed the successful modification of alkyl chains on the HMS. Compared to the spectrum of HMS/C18, a new C=O bond (1740 cm^{-1}) appeared in the spectrum of DOX/HMS/C18, suggesting that DOX molecules were loaded into the nanoparticles successfully.

Assembly of HMS/C18/PRMS-FA

The folate conjugated amphiphilic copolymer PRMS-FA was coated onto HMS nanoparticles *via* self-assembly. After modification with C18 alkyl chains, the surface of HMS nanoparticles became hydrophobic. The hydrophobic part of the PRMS-FA associates with the hydrophobic C18 alkyl chains through hydrophobic van der Waals interactions during the self-assembly process, as a result the amphiphilic copolymer PRMS-FA was coated onto the surface of the HMS nanoparticles successfully. The detailed morphological features of the nanoparticles were determined by TEM.

As shown in Fig. 3, after the pure HMS was modified with C18, no significant changes were observed and the pores in the silica shell remained clearly visible, suggesting that the modification with C18 does not affect the porosity of HMS. After self-assembly with PRMS-FA, the profile of HMS/C18/PRMS-FA became blurred and a thick layer of polymer film could be clearly observed. After UV ($\lambda = 365$ nm) irradiation, the

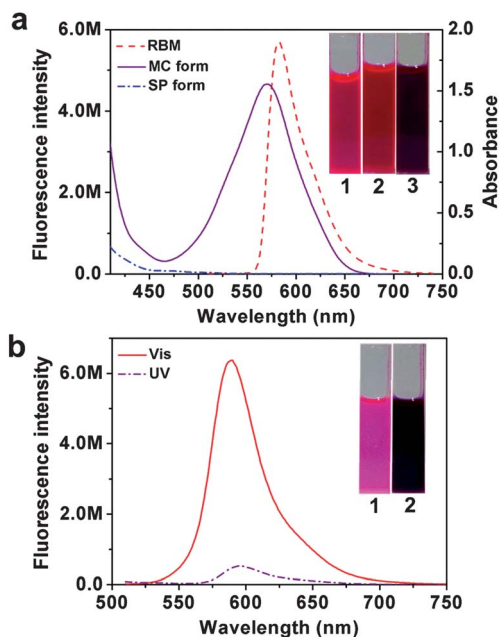


Fig. 1 (a) Superposition of the fluorescence emission of rhodamine B (2-hydroxyethyl acrylate) ester (RBM) and the absorbance of SPMA before (SP form) and after (MC form) UV irradiation (the inset images show photographs of the RBM solution (1), mixed solution of RBM and SPMA before (2) and after (3) UV irradiation); (b) fluorescence spectra of the light-responsive copolymer PRMS-FA before and after UV ($\lambda = 365$ nm) irradiation (the inset images show photographs of PRMS-FA solution under visible light irradiation (1) and UV irradiation (2)).

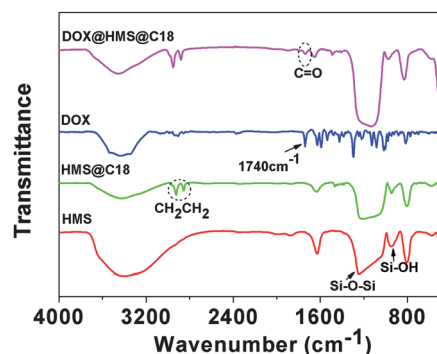


Fig. 2 FTIR spectra of HMS, HMS/C18, DOX and DOX/HMS/C18.

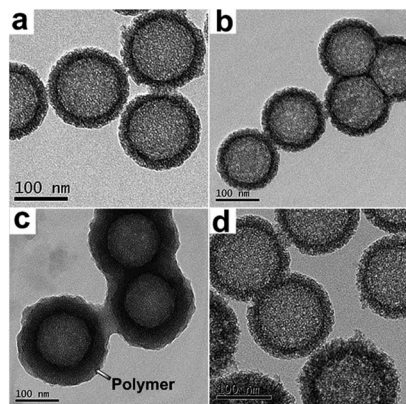


Fig. 3 TEM images of HMS (a), HMS/C18 (b), HMS/C18/PRMS-FA (c) and HMS/C18/PRMS-FA upon UV irradiation (d).

copolymer layer disappeared which confirmed our previous thought. Furthermore, the DLS result (Fig. S3†) showed that the nanoparticles gained an average diameter of 200 nm after modification with the copolymer which corresponded to the TEM images.

Drug loading and release

DOX was chosen as a model anti-cancer drug to discuss the drug loading and release behaviour of PRMS-FA/HMS/C18. DOX was first loaded into the hollow core of HMS/C18. The N_2 adsorption/desorption isotherms of HMS, HMS/C18 and DOX/HMS/C18 (Fig. S4†) indicated that the modification of C18 and loading of DOX molecules had little influence on the pore structure of the HMS, which is significant for drug loading and release. The drug loading content was determined by measuring the DOX concentration before and after loading the HMS/C18. The theoretical loading content was set at 5%, 10% and 50%, respectively and the DOX loading efficiency was measured as 74.6, 73.4 and 66.8% accordingly (Table 1). It was obvious that HMS had higher drug loading content and efficiency than common mesoporous silica due to its hollow core.

The DOX-loaded HMS/C18 was coated with the copolymer PRMS-FA *via* a self-assembly process to obtain DOX/HMS/C18/PRMS-FA. And the results of DOX release from HMS/C18 and HMS/C18/PRMS-FA indicated that the copolymer layers could block the nanopores of HMS to cage the pre-loaded drugs (Fig. S5†).

Table 1 Drug loading content and drug loading efficiency of HMS/C18

Theoretical drug loading content (wt%)	Drug loading content ^a (wt%)	Drug loading efficiency (%)
5	3.73	74.6
10	7.34	73.4
50	33.4	66.8

^a Drug loading content for DOX was determined by UV-Vis spectroscopy.

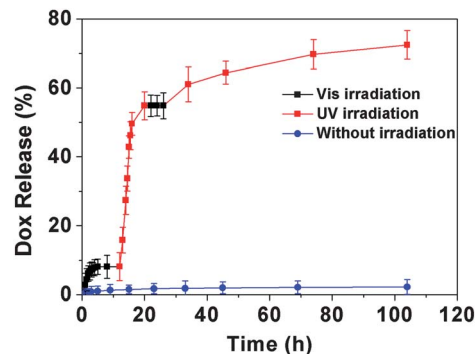


Fig. 4 Release of DOX *in vitro* from HMS/C18/PRMS-FA with and without light irradiation at 37 °C.

The results of drug release from HMS/C18/PRMS-FA *in vitro* are shown in Fig. 4. DOX-loaded HMS/C18/PRMS-FA was first immersed in PBS at 37 °C. Upon visible light irradiation for 8 h, less than 10 wt% of DOX was released. There was almost no further release after another 4 h irradiation. However, a fast and high release of DOX was measured after the nanocarrier was irradiated with UV light ($\lambda = 365$ nm). No further release of DOX was measured after visible light irradiation for 4 h. The process of drug release continued upon UV irradiation and approximately 70 wt% of DOX was released within 100 h. There was negligible release of DOX when the nanocarrier was placed in the dark. These results confirmed that DOX/HMS/C18/PRMS-FA would only release drugs after irradiation with UV light.

Evaluation of cytotoxicity and cell uptake

The sulforhodamine B (SRB) assay was used to assess the cytotoxicity of the nanocarrier. After incubation with the nanocarrier for 72 h, the cells displayed high cell viability (>80%) as shown in Fig. 5. Even at a high concentration, the cytotoxicity still remained at a low level, which is significant for the later experiment *in vitro*. The results above proved that the polymer shell was biocompatible. These characteristics are necessary for further biomedical application.

To investigate the properties of HMS/C18/PRMS-FA nanocarriers in tumor cell targeting and cell imaging, the cellular uptake of nanocarriers by FR(+) and FR(-) cells was measured.

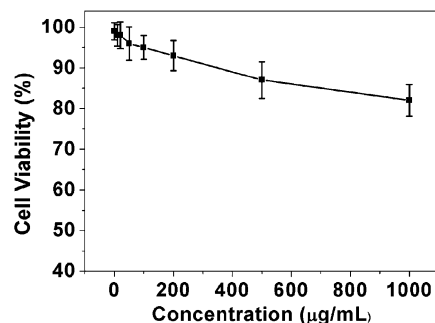


Fig. 5 *In vitro* cell viability of HMS/C18/PRMS-FA at different concentrations.

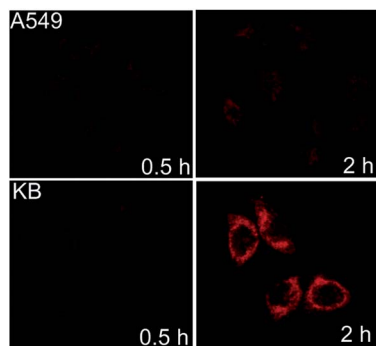


Fig. 6 CLSM of FR (–) A549 cells and FR (+) KB cells incubated with DOX/HMS/C18/PRMS-FA for 0.5 h and 2 h.

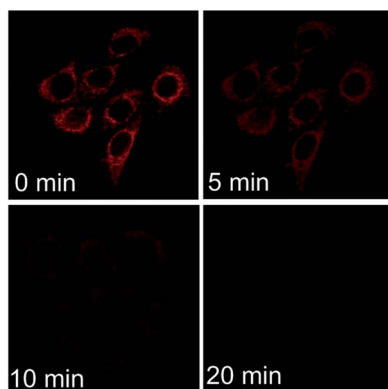


Fig. 7 CLSM observations of the FRET process.

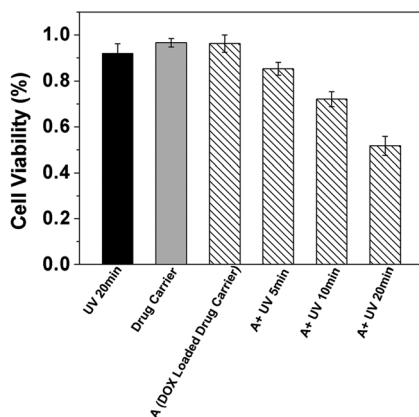


Fig. 8 Inhibition of KB cell growth in the presence of excitation at 365 nm (20 min), drug carrier HMS/C18/PRMS-FA and DOX loaded drug carrier without or with UV light exposures for varying durations after 24 h of incubation.

The confocal laser scanning microscopy (CLSM) images of cells with DOX/HMS/C18/PRMS-FA solution at different incubation times are shown in Fig. 6. After 0.5 h, there was no significant difference in fluorescence intensity between the two nanocarriers. However, a significant increase in fluorescence intensity can be observed in KB cells incubated with FA-conjugated

nanocarriers after 2 h. The changes in fluorescence intensity suggested that the targeting moiety offered by folic acid is efficient at enhancing tumor cell targeting *in vitro*. The high fluorescence intensity of the nanocarriers ensures their application can be utilized in fluorescence imaging.

Observation of the FRET process in cancer cells by CLSM

We investigated use of the FRET property for monitoring the light-controlled drug release from the nanocarriers by confocal laser scanning microscopy (CLSM). We incubated the DOX-loaded nanocarriers ($500 \mu\text{g mL}^{-1}$) with KB cells for 2 h in the dark at first. Then the cells were exposed to UV light ($\lambda = 365 \text{ nm}$, 0.2 W cm^{-2}) for time periods ranging from 0 to 20 minutes and the cells were examined by CLSM. As can be seen from Fig. 7, a strong red emission excited at 510 nm was visible in the KB cells without UV irradiation while the fluorescence intensity decreased gradually with as the UV irradiation time increased. The mean fluorescence intensity of cancer cells is shown in Fig. S6.† We attributed the change in fluorescence intensity to the structure conversion of the light-responsive copolymer in the nanocarriers, resulting in the FRET process. Since the structure conversion would make the light-responsive copolymer break away from the HMS nanoparticles, triggering the drug release, the FRET process combined with the light-controlled drug release has the ability to be a real-time monitor.

The *in vitro* cytotoxicity of DOX/HMS/C18/PRMS-FA under UV irradiation was evaluated using the MTT assay. We incubated KB cells in a culture medium with DOX/HMS/C18/PRMS-FA under UV irradiation, and with HMS/C18/PRMS-FA, DOX/HMS/C18/PRMS-FA, and a blank sample under UV irradiation as the controls. After 3 h of incubation, the nanocarriers were removed and the cells were incubated for another 24 h in the dark. As can be seen in Fig. 8, treatment with UV light at a low power did not result a significant decrease in the cell viability. The cells still kept high viability after being treated with DOX/HMS/C18/PRMS without UV irradiation, indicating no DOX was released without irradiation. In contrast, DOX/HMS/C18/PRMS-FA under UV irradiation within 20 minutes showed an obviously enhanced cytotoxicity to the KB cells, which could be explained by the light controlled drug release.

Conclusion

In summary, we have prepared a core-shell nanocomposite as nanocarrier and real-time monitor for light controlled drug delivery *via* a facile strategy. HMS, an ideal base material with good biocompatibility, was introduced into the nanocarrier to enhance its drug loading capability and stability. By introducing selective targeting folate groups to the copolymer, the nanocarrier could target into FR(+) KB cells. The UV light ($\lambda = 365 \text{ nm}$) could make the amphiphilic copolymer shell become hydrophilic and separate from the hydrophobic surface of the HMS nanoparticles, resulting in a significant amount of drug release (>70%) to inhibit the cancer cells. Moreover, a FRET process based on the transformation of the copolymer occurred simultaneously with

the drug release process which could provide an approach to monitor the light-triggered drug release in real time. *In vitro* studies confirmed the biocompatibility and the efficacy of this nanocarrier for cancer cell targeting and inhibition, which guarantees it a potential biomedical application.

Acknowledgements

We gratefully acknowledge the financial support provided by National Natural Science Foundation of China (21176164, 21301125), Natural Science Foundation of Jiangsu Province (BK2012625), Natural Science Foundation of the Jiangsu Higher Education Institutions of China (13KJB430022), a project funded by the Priority Academic Program Development of Jiangsu Higher Education Institutions (PAPD) and Joint Research Projects of SUN-WIN Joint Research Institute for Nanotechnology.

Notes and references

- (a) E. Fleige, M. A. Quadir and R. Haag, *Adv. Drug Delivery Rev.*, 2012, **64**, 866; (b) J. Nicolas, S. Mura, D. Brambilla, N. Mackiewicz and P. Couvreur, *Chem. Soc. Rev.*, 2013, **42**, 1147; (c) Q. He and J. L. Shi, *J. Mater. Chem.*, 2011, **21**, 5845; (d) Q. He, Y. Gao, L. X. Zhang, W. B. Bu, H. R. Chen, Y. P. Li and J. L. Shi, *J. Mater. Chem.*, 2011, **21**, 15190.
- (a) X. Mei, S. Yang, D. Y. Chen, N. J. Li, H. Li, Q. F. Xu, J. F. Ge and J. M. Lu, *Chem. Commun.*, 2012, **48**, 10010; (b) D. Schmaljohann, *Adv. Drug Delivery Rev.*, 2006, **58**, 1655; (c) S. Sortino, *J. Mater. Chem.*, 2012, **22**, 301.
- (a) C. Brieke, F. Rohrbach, A. Gottschalk, G. Mayer and A. Heckel, *Angew. Chem., Int. Ed.*, 2012, **51**, 8446; (b) Y. Zhao, *Macromolecules*, 2012, **45**, 3647; (c) Y. Zhao, *J. Mater. Chem.*, 2009, **19**, 4887; (d) G. Pasparakis, T. Manouras, P. Argitis and M. Vamvakaki, *Macromol. Rapid Commun.*, 2012, **33**, 183.
- (a) J. Liu, W. Bu, L. Pan and J. L. Shi, *Angew. Chem., Int. Ed.*, 2013, **52**, 1; (b) M. L. Viger, M. Grossman, N. Fomina and A. Almutairi, *Adv. Mater.*, 2013, **25**, 3733; (c) X. J. Yang, Q. Q. Xiao, C. X. Niu, N. Jin, J. Ouyang, X. Y. Xiao and D. C. He, *J. Mater. Chem. B*, 2013, **1**, 2757.
- (a) F. Ercole, T. P. Davis and R. A. Evans, *Polym. Chem.*, 2010, **1**, 37; (b) Y. Wang, C. Y. Hong and C. Y. Pan, *Biomacromolecules*, 2012, **13**, 2585; (c) H. Zhao, E. S. Sterner, E. B. Coughlin and P. Theato, *Macromolecules*, 2012, **45**, 1723.
- (a) F. D. Jochum and P. Theato, *Chem. Commun.*, 2010, **46**, 6717; (b) H. Lee, W. Wu, J. K. Oh, L. Mueller, G. Sherwood, L. Peteanu, T. Kowalewski and K. Matyjaszewski, *Angew. Chem., Int. Ed.*, 2007, **46**, 2453; (c) S. Kumar, J. F. Allard, D. Morris, Y. L. Dory, M. Lepage and Y. Zhao, *J. Mater. Chem.*, 2012, **22**, 7252.
- (a) C. Huang, K. G. Neoh, E. T. Kang and B. Shuter, *J. Mater. Chem.*, 2011, **21**, 16094; (b) S. J. Zhu, L. L. Qian, M. H. Hong, L. H. Zhang, Y. Y. Pei and Y. Y. Jiang, *Adv. Mater.*, 2011, **23**, H84; (c) G. J. L. Bernardes, G. Casi, S. Trüssel, I. Hartmann, K. Schwager, J. Scheuermann and D. Neri, *Angew. Chem., Int. Ed.*, 2012, **51**, 941.
- (a) N. C. Fan, F. Y. Cheng, J. A. Ho and C. S. Yeh, *Angew. Chem., Int. Ed.*, 2012, **51**, 8806; (b) T. Lammers, F. Kiessling, W. E. Hennink and G. Storm, *J. Controlled Release*, 2012, **161**, 175.
- (a) C. Brieke, F. Rohrbach, A. Gottschalk, G. Mayer and A. Heckel, *Angew. Chem., Int. Ed.*, 2012, **51**, 8446; (b) B. Liao, P. Long, B. Q. He, S. J. Yi, B. L. Ou, S. H. Shen and J. Chen, *J. Mater. Chem. C*, 2013, **1**, 3716; (c) J. Allouche, A. L. Beulze, J. C. Dupin, J. B. Ledeuil, S. Blanc and D. Gonbeau, *J. Mater. Chem.*, 2010, **20**, 9370.
- J. P. Lai, B. P. Shah, E. Garfunkel and K. B. Lee, *ACS Nano*, 2013, **7**, 2741.
- F. May, M. Peter, A. Hütten, L. Prodi and J. Mattay, *Chem.–Eur. J.*, 2012, **18**, 814.
- (a) A. Rösler, G. W. M. Vandermeulen and H. A. Klok, *Adv. Drug Delivery Rev.*, 2012, **64**, 270; (b) W. L. Yang and B. S. Li, *J. Mater. Chem. B*, 2013, **1**, 2525.
- (a) X. Mei, D. Y. Chen, N. J. Li, Q. F. Xu, J. F. Ge, H. Li, B. X. Yang, Y. J. Xu and J. L. Lu, *Soft Matter*, 2012, **8**, 5309; (b) B. Yan, J. Christopher, N. R. Branda and Y. Zhao, *J. Am. Chem. Soc.*, 2011, **133**, 19714; (c) D. Y. Chen, N. J. Li, H. W. Gu, X. W. Xia, Q. F. Xu, J. F. Ge, J. M. Lu and Y. G. Yang, *Chem. Commun.*, 2010, **46**, 6708.
- (a) P. P. Yang, S. L. Gai and J. Lin, *Chem. Soc. Rev.*, 2012, **41**, 3679; (b) L. Xing, H. Q. Zheng, Y. Y. Cao and S. N. Che, *Adv. Mater.*, 2012, **24**, 6433; (c) S. K. Das, M. K. Bhunia, D. Chakraborty, A. R. Khuda-Bukhsh and A. Bhaumik, *Chem. Commun.*, 2012, **48**, 2891.
- S. Yang, D. Y. Chen, N. J. Li, X. Mei, X. X. Qi, H. Li, Q. F. Xu and J. M. Lu, *J. Mater. Chem.*, 2012, **22**, 25354.
- G. Qi, Y. B. Wang, L. Estevez, A. K. Switzer, X. N. Duan, X. F. Yang and E. P. Giannelis, *Chem. Mater.*, 2010, **22**, 2693.
- T. Wu, G. Zou, J. M. Hu and S. Y. Liu, *Chem. Mater.*, 2009, **21**, 3788.
- D. M. Mizrahi, M. Omer-Mizrahi, J. Goldshtein, N. Askinadze and S. Margel, *J. Polym. Sci., Part A: Polym. Chem.*, 2010, **48**, 5468.
- E. S. Lee, K. T. Oh, D. Kim, Y. S. Youn and Y. H. Bae, *J. Controlled Release*, 2007, **123**, 19.